Quantum Monte Carlo study of the disordered attractive Hubbard model

R. T. Scalettar
Department of Physics, University of California, Davis, California 95616

N. Trivedi
Theoretical Physics Group, Tata Institute for Fundamental Research, Mumbai 400005, India

C. Huscroft
Department of Physics, University of California, Davis, California 95616

(Received 2 July 1998)

We investigate the disorder-driven superconductor to insulator quantum phase transition (SIT) in an interacting *fermion* model using determinantal quantum Monte Carlo (QMC) methods. The disordered superconductor is modeled by an attractive Hubbard model with site disorder chosen randomly from a uniform distribution. The superconducting state which exists for small disorder is shown to evolve into an insulating phase beyond a critical disorder. The transition is tracked by the vanishing of (a) the superfluid stiffness, and (b) the charge stiffness or the delta function peak in the optical conductivity at zero frequency. We also show the behavior of the charge, spin, pair, and current correlations in the presence of disorder. Results for the temperature dependence of the dc conductivity, obtained by an approximate analytic continuation technique, are also presented both in the metallic phase above T_c and the insulating phase. We discuss some of the complications in extracting the resistance at the transition point. [S0163-1829(99)00306-9]

I. INTRODUCTION

In a wide variety of two-dimensional disordered systems,[1] from granular and homogeneously disordered Bi, Pb, and Sn films,[2–4] to $In_{1-x}O_x$ (Ref. 5) and MoGe films,[6] high-temperature superconducting films[7,8] and Josephson-junction arrays,[9] a transition from a superconductor to an insulator (SIT) can be driven by adjusting some tuning parameter such as the film thickness, the O concentration, the magnetic-field strength, or the charging energy. The experimental signature of the transition is that the behavior of the sheet resistance $R_\square(T)$ as a function of temperature T is different in the two phases. At low disorder or magnetic field, the system is superconducting for $T<T_c$. The transition temperature T_c decreases with increasing disorder or magnetic field and above T_c the system is metallic with $dR_\square/dT>0$. Beyond a critical disorder or magnetic field, on the other hand, the system becomes insulating with $dR_\square/dT<0$.

Motivated by these experiments, one of the important open theoretical questions is to study particular microscopic models to see whether or not they show a SIT as a function of some tuning parameter such as the degree of disorder and, if so, characterize the transition.

Anderson[10] proposed that the superconducting transition temperature T_c and the thermodynamic properties should be *unaffected* by disorder since Cooper pairs can be formed by pairing the time-reversed exact eigenstates of the noninteracting disordered problem. This is only valid for small disorder in the regime $k_F l \gg 1$, where k_F is the Fermi momentum and l is the elastic mean free path. Ma and Lee[11] developed a mean-field theory in which they assumed that the order parameter was uniform throughout the system. As a consequence, the superfluid density remained large even for fairly high disorder and was found to persist essentially all the way to the site-localized limit.

One might therefore ask whether a disorder-driven SIT can occur at all. It is important to note that both the Anderson and Ma-Lee arguments make specific assumptions concerning the effect of randomness, and hence may not be compelling in all cases. In order to understand why a SIT might be possible, consider the two generic mechanisms for the destruction of superconductivity. First, the magnitude of the pairing gap can be driven to zero. Second, phase coherence between the pairs in different parts of the sample may be lost. Clearly there is an interplay between fluctuations in the pair amplitude and phase. For example, the phase can change at a smaller energy cost in regions where the amplitude is lower.[12] It is possible that the pair amplitude is driven to zero at the same point where phase coherence is lost, but it is also possible that the two phenomena occur separately.

Fisher and collaborators[13] were the first to describe a scenario in which phase fluctuations caused a SIT while the pair amplitude remained finite. They conjectured that the SIT might be in the same universality class as the superfluid-insulator transition for bosons. They argued that since near the transition the size of the Cooper pair is much smaller than the diverging correlation length, it is possible to describe it as a Bose field. Of course, the charge carriers of the experimental systems are fermionic in nature, so it is useful to study Hamiltonians that do not begin immediately with bosonic degrees of freedom. Perturbative methods to study the SIT in fermionic models have not been successful in describing the transition region,[14,15] which is not surprising since the transition occurs in a region of high disorder in an interacting system.

While this approach has led to a number of very interesting results, especially for the value of the conductivity at the transition,[16–19] it is important to test the validity of the phase-

only models by developing methods that also treat amplitude fluctuations. In order to better describe the behavior of a superconductor at high disorder, Ghosal, Randeria, and Trivedi[20] have included the fluctuations of the superconducting order parameter by solving the ''Bogoliubov–de Gennes'' mean-field equations self-consistently. They have found that the probability distribution of the local pairing amplitude develops a broad distribution with significant weight near zero with increasing disorder. Surprisingly, the density of states continues to show a finite spectral gap, as also seen by quantum Monte Carlo (QMC) and maximum entropy techniques,[21] shown to arise from the breakup of the system into superconducting islands separated by regions with very small pairing amplitude. These disorder-induced fluctuations in the order-parameter amplitude have a marked effect in suppressing the superfluid density at higher disorder but by themselves are not sufficient to drive the system nonsuperconducting. It is necessary to include phase fluctuations distributed inhomogeneously riding on top of the highly inhomogeneous amplitude fluctuations to get a SIT.

In this paper we describe the first QMC study of a fermion model of superconductivity (the attractive Hubbard Hamiltonian with random-site energies) that gives a SIT at a critical disorder strength.[22] The attractive Hubbard Hamiltonian that we study is a simple model of a disordered superconductor (SC) that allows us to explore the qualitative issues arising from the interplay of superconductivity and localization. While such a model does not address questions concerning the microscopic origin of the pairing, since the attraction is put in *a priori*, one can nevertheless examine questions such as the competition between superconductivity and charge-density-wave formation,[23] the behavior of superconducting correlations above the superconducting transition temperature,[24–28] and the interpolation between weak-coupling BCS and strong-coupling bosonic regimes of pair formation.[29]

II. ORGANIZATION OF THE PAPER

This paper is organized as follows: In Sec. III we introduce the attractive Hubbard model and briefly review the physics of the clean attractive Hubbard model. In Sec. IV we describe the QMC simulation technique. In Sec. V we first discuss our results for the chemical potential in order to demonstrate that we are in the degenerate Fermi regime of the model. We then describe the effect of disorder on the local and longer range density-density and pairing correlations. The pairing correlations are found to be much more robust compared to the density correlations away from half filling. We also show the behavior of the superconducting order parameter that decreases rapidly with increasing disorder and vanishes beyond a critical disorder. In Sec. VI we present a detailed discussion of the longitudinal and transverse current-current correlation functions. The longitudinal response obeys the *f*-sum rule and equals the absolute value of half the lattice kinetic energy K_x that we verify in our simulations. The transverse response, on the other hand, deviates from K_x and this deviation is a measure of the superfluid stiffness of the system. We present results showing the suppression of the superfluid stiffness with disorder and its ultimate destruction beyond a critical disorder. In Sec. VII we discuss the behavior of the frequency dependent current-current correlation function and the extraction of the charge stiffness or the strength of the delta-function peak in the optical conductivity. Our results show that in the superconducting phase the superfluid stiffness and the charge stiffness are roughly equal in magnitude for all disorder strengths. In Sec. VIII we discuss an approximate method to extract the temperature dependence of the dc resistivity and show its behavior in the metallic phase above T_c for low disorder as well as in the insulating phase for higher disorder. The resistivity at the transition is extracted by two methods. (i) At the critical disorder, the charge stiffness vanishes with frequency with a slope proportional to the resistivity; and (ii) from the crossing of the resistivity vs disorder curves at various temperatures. We also discuss the complications of obtaining the resistivity near a quantum critical point. We present our conclusions in Sec. IX and end with some of the outstanding questions in the area of SIT in Sec. X. In previous papers[22,30,31] we have presented a short discussion of some of these issues. The purpose of the present paper is to provide the details behind that work, as well as to present a number of new results including a more complete discussion of both the physics and the numerics.

III. MODEL

The Hamiltonian we study is defined by

$$H = -t\sum_{\langle \mathbf{ij}\rangle\sigma}(c^{\dagger}_{\mathbf{i}\sigma}c_{\mathbf{j}\sigma}+c^{\dagger}_{\mathbf{j}\sigma}c_{\mathbf{i}\sigma}) - \sum_{\mathbf{i}\sigma}(\mu - V_{\mathbf{i}})n_{\mathbf{i}\sigma} - |U|\sum_{\mathbf{i}}(n_{\mathbf{i}\uparrow}-\tfrac{1}{2})(n_{\mathbf{i}\downarrow}-\tfrac{1}{2}). \quad (1)$$

Here the lattice sum $\langle \mathbf{ij}\rangle$ is over nearest-neighbor sites on a two-dimensional square lattice, $c_{\mathbf{i}\sigma}$ is a fermion destruction operator at site $\mathbf{i}$ with spin σ, $n_{\mathbf{i}\sigma}=c^{\dagger}_{\mathbf{i}\sigma}c_{\mathbf{i}\sigma}$, and the chemical potential μ fixes the average density $\langle n\rangle$. The site energies $V_{\mathbf{i}}$ are independent random variables with a uniform distribution over $[-V/2,V/2]$. The interaction has been written in particle-hole symmetric form so that $\mu=0$ corresponds to $\langle n\rangle=1$ at all U and T when $V=0$. We set $t=1$ and measure all energies in units of t.

In real materials, disorder plays a complicated role in the Hamiltonian, both affecting the screening of the electron-electron interaction as well as the phonons and hence the electron-phonon interaction. Our Hamiltonian does not include these effects.

Some of the physics of the clean attractive Hubbard model may be summarized as follows:[32,33] At half filling ($\mu=0$), the model has no long-range correlations at any finite temperature, and at $T=0$ is in a state with combined charge density wave (CDW) and superconducting order.[34] When $\mu\neq 0$ the system has a finite-temperature Kosterlitz-Thouless transition to a state with superconducting order. The transition temperature T_c depends strongly on the filling near $\langle n\rangle=1$. T_c shows a nonmonotonic dependence on coupling[29] similar to the repulsive Hubbard model where the Néel temperature first increases with U but then goes down as $T_N \propto J = 4t^2/U$ at strong coupling. Numerical

estimates[35,36] of T_c are still a matter of considerable debate and at $\langle n\rangle = 0.875$ vary from $0.3t$ to $0.03t$.

IV. QUANTUM MONTE CARLO SIMULATION

Our simulation uses the standard ''determinant'' QMC algorithm,[37,38] along with its various refinements.[39,40] The partition function $Z = \mathrm{Tr}[e^{-\beta H}]$ is written as a path integral by discretizing the imaginary time dimension $\beta = 1/T$ into N_τ time slices as

$$e^{-\beta H} = (e^{-\Delta\tau H})^{N_\tau} \approx (e^{-\Delta\tau H_1} e^{-\Delta\tau H_U})^{N_\tau}, \tag{2}$$

where $\beta = N_\tau \Delta\tau$. In Eq. (2), H_1 is the sum of the two single-particle terms in Eq. (1) and H_U is the interaction term. A systematic Trotter error is introduced in Eq. (2) because of the noncommutativity of the operators H_1 and H_U. This Trotter error, however, can be dealt with, either by making $\Delta\tau$ sufficiently small so that errors in observables are of the same order as statistical fluctuations from the sampling, or, if greater accuracy is needed, by extrapolating to $\Delta\tau = 0$. The exponential of the interaction term is decoupled using a Hubbard-Stratonovich (HS) transformation by introducing a discrete field[41] $S_{i\tau} = \pm 1$ at each point in the space-time lattice,

$$\exp[+\Delta\tau |U| (n_{i\uparrow} - 1/2)(n_{i\downarrow} - 1/2)] = \frac{1}{2}\exp\left\{\frac{-\Delta\tau |U|}{4}\right\} \sum_{S_{i\tau}=\pm 1} \exp[\Delta\tau\lambda S_{i\tau}(n_{i\uparrow} + n_{i\downarrow} - 1)], \tag{3}$$

where

$$\cosh(\Delta\tau\lambda) = \exp(\Delta\tau |U|/2) \tag{4}$$

is satisfied by *real* λ. Thus the original functional integral over Grassman variables, which involved traces containing *quartic* operators is reduced to a quadratic problem in the fermion operators *but at the cost of performing a sum over all configurations of the HS fields on the discretized space-time lattice*. The partition function in the grand canonical ensemble is

$$Z = \mathrm{Tr}\exp\{-\beta H\} = \sum_{\{S\}} \mathrm{Tr} \prod_{\tau,\sigma} \exp\left[-\Delta\tau \sum_{i,j} c^\dagger_{i\sigma} h_{\{S\}}(\tau,\sigma) c_{j\sigma}\right]. \tag{5}$$

Here $h_{\{S\}}(\tau,\sigma)$ is a one-body Hamiltonian for the motion of an electron in a given configuration of the HS fields. Note in Eq. (3) both the up and down electrons couple to the HS field with the *same* sign.

Now the resulting trace over quadratic forms in the fermion operators in Eq. (5) is performed and gives

$$Z = \sum_{\{S\}} \det M_\uparrow(\{S\}) \det M_\downarrow(\{S\}) \tag{6}$$

with

$$M_\sigma(\{S\}) = \left[I + \prod_\tau e^{-\Delta\tau h_{\{S\}}(\tau,\sigma)}\right]. \tag{7}$$

Thus the interacting problem is equivalent to solving a non-interacting problem for a given HS field configuration $\{S_{i\tau}\}$ and then summing over all possible configurations. The sum over the HS fields on the space-time lattice is efficiently done using Monte Carlo techniques that generate the configurations, treating the product of the determinants as a probability. Note that in general for a fermion problem, since the sign of the determinants may be negative, the product is not necessarily non-negative and it cannot be treated as a probability. This is the origin of the ''sign problem'' for typical fermion problems. However, for the Hamiltonian in Eq. (1), since it is possible to couple the HS field to the charge $n_{i\uparrow} + n_{i\downarrow}$ and satisfy Eq. (4) with real λ, the two determinants in Eq. (6) are *identical*, and hence the integrand is non-negative, thus there is no sign problem[41] in attractive Hubbard model simulations *at any filling*.

In the determinant QMC approach, finite-temperature expectation values of combinations of fermion operators with arbitrary space and imaginary time arguments can be easily evaluated. More precisely, if all the operators are at the same imaginary time, the observables can be expressed in terms of matrix elements of the inverse of the matrices whose determinants give the Boltzmann weight. These matrix elements are needed to update the HS field, and are therefore available ''free of charge'' for the measurements. If the operators whose expectation values are to be measured have different imaginary time arguments, some extra calculations are involved to obtain the nonequal-time Green's functions. However, this can be done in a straightforward manner.[37,39,40]

V. EQUAL-TIME CORRELATIONS

A. Chemical potential

The location of the chemical potential relative to the bottom of the band gives information about the degeneracy of the system. In the simulations presented in this paper the filling is chosen to be $\langle n\rangle = 0.875$ close to the point where T_c is expected to be maximal for $U = -4t$.[35] For a given value of the parameters—interaction strength U, disorder strength V, and temperature T—the chemical potential μ is tuned so that upon disorder averaging the density $\langle n\rangle \sim 0.875$. We comment that an alternative approach is to tune the chemical potential for each disorder realization separately so that each has the same desired filling. This is likely to result in reduced fluctuations,[42] but is considerably more time consuming numerically. Some such approach, however, appears essential for analytic continuation calculations.[21]

The dependence of μ on V is roughly linear and is shown in Fig. 1 for $U = -4t$. Since μ, measured from the bottom of the band and taking into account the Hartree shift, is larger than the temperature, $\mu(T, |U|, V) + 4t + \langle n\rangle |U|/2 > T$, the system is degenerate and far from the regime where there are preformed bosons. Note, we have assumed that the bottom of the band is at $-4t$, which is the case in the clean system but should be renormalized by the random potential in the disordered system.

B. Density-density correlations

In Fig. 2 we show the double occupancy $\langle \mathbf{n_{i\uparrow} n_{i\downarrow}} \rangle$ that is found to increase from 0.32 at $V = 0$ to 0.38 at $V = 5$. This

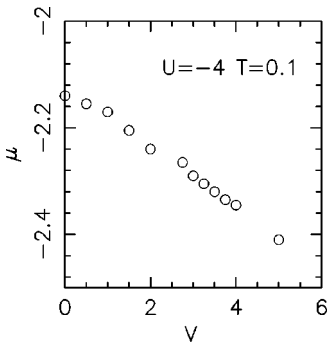

FIG. 1. The chemical potential μ shows a roughly linear decrease with disorder V. Since $\mu(T,|U|,V)+4t+\langle n\rangle|U|/2\sim 3.5t \gg T$ the system is in a highly degenerate regime and away from the preformed bosonic regime.

increase is a consequence of the fact that in the attractive model, random-site energies and interactions both act to promote double occupancy, in contrast to the repulsive model where they compete.

In Figs. 3(a) and 3(b) we also show the spatial variation of the density-density correlation function

$$C_{\sigma,\sigma'}(\mathbf{l})=\langle \mathbf{n_{i\sigma}n_{i+l,\sigma'}}\rangle-\langle \mathbf{n_{i\sigma}}\rangle\langle \mathbf{n_{i+l,\sigma'}}\rangle. \tag{8}$$

At half filling, $C(\mathbf{l})$ is rapidly suppressed by disorder;[23] via finite-size scaling it is seen that even as little disorder as $V=0.25t$ is capable of destroying the charge-density-wave ordering and in an 8×8 system $C(\mathbf{l})$ is definitely suppressed by $V=1t$. Away from half filling even for the clean system $C(\mathbf{l})$ is small and thereafter disorder does not have any further effect.

C. Pair correlations

An important characteristic of the superconducting state is that the equal-time s-wave pair-correlation function P_s defined by

$$P_s(\mathbf{l})=\langle \Delta_{\mathbf{i}}\Delta^{\dagger}_{\mathbf{i+l}}\rangle,$$
$$\Delta^{\dagger}_{\mathbf{i}}=c^{\dagger}_{\mathbf{i}\uparrow}c^{\dagger}_{\mathbf{i}\downarrow}, \tag{9}$$

has a finite value at large separations $P_s[\mathbf{l}=(L/2,L/2)]=\Delta^2_{OP}$, where Δ_{OP} is the ''order parameter'' on a lattice of finite size L.

In Fig. 4 we show the behavior of P_s at a temperature T

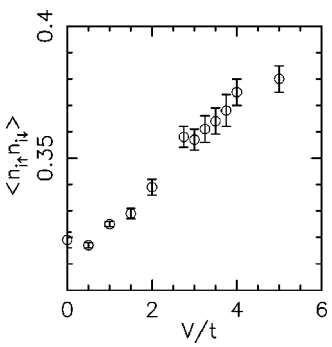

FIG. 2. The increase in double occupancy $\langle \mathbf{n_{i\uparrow}n_{i\downarrow}}\rangle$ as a function of increasing disorder V/t.

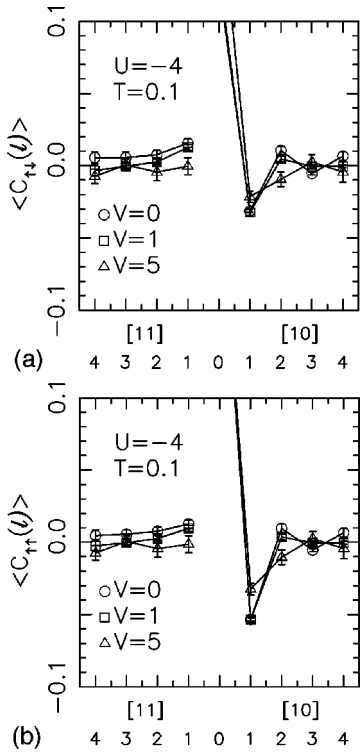

FIG. 3. The density correlation function $C_{\sigma,\sigma'}(\mathbf{l})$ from Eq. (8) for $\mathbf{l}$ along [10] and [11] directions for (a) $(\sigma,\sigma')=(\uparrow,\downarrow)$ and (b) $(\sigma,\sigma')=(\uparrow,\uparrow)$, showing rapid suppression with increasing disorder.

$=0.1t$ for varying degrees of disorder. This temperature is sufficiently low that for the clean system the correlation length has exceeded the linear lattice size and the system is effectively in the ground state. For the clean system, or weak disorder, the correlation function approaches a constant at large distances, implying a SC state with long-range order. For strong disorder, the correlation function vanishes at large distances indicating the absence of an order parameter. It is evident by comparison with Fig. 3 that pairing correlations are much more robust than density-density correlations for the same degree of disorder, as in the half-filled case.[23]

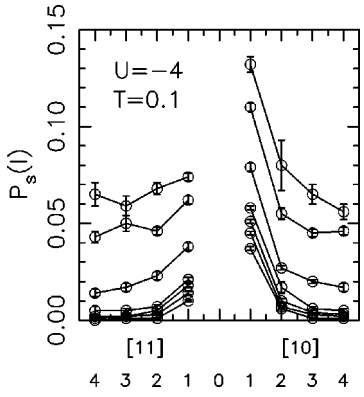

FIG. 4. The pair-correlation function defined in Eq. (9) is shown as a function of $\mathbf{l}$, the relative separation of the two sites along [10] and [11] directions for varying disorder strengths $V=0$, 1.0, 2.0, 3.0, 3.5, 4.0, and 5.0. The value at $\mathbf{l}=0$ is given by Eq. (10) but is not shown as it is off-scale. Note the relative robustness of the pairing correlations compared to the density correlations in Fig. 3 in the presence of disorder.

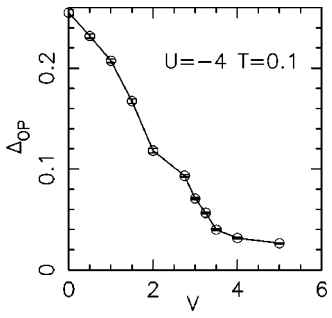

FIG. 5. Suppression of the superconducting ''order parameter'' Δ_{OP} on an 8×8 lattice with increasing disorder. While Δ_{OP} does not vanish at large V due to finite-size effects, a scaling analysis of the pair structure factor indicates that in the thermodynamic limit Δ_{OP} vanishes around a critical disorder $V_c\sim3.5t$.

Figure 5 shows the order parameter Δ_{OP} as a function of disorder that is strongly suppressed by disorder and vanishes beyond a critical disorder strength $V_c\sim3.5t$.

The value of the pairing correlation function at zero separation is related to the occupancy and double occupancy,

$$P_s(\mathbf{0})=\langle\Delta_{\mathbf{i}}\Delta_{\mathbf{i}}^{\dagger}\rangle=1-\langle n\rangle+\langle n_{i\uparrow}n_{i\downarrow}\rangle. \tag{10}$$

Whereas $P_s(\mathbf{l})$ is reduced by disorder for $\mathbf{l}$ nonzero, $P_s(\mathbf{0})$ is increased, since the density $\langle n\rangle$ is fixed and the double occupancy rate $\langle n_{i\uparrow}n_{i\downarrow}\rangle$ is increased (Fig. 2).

The equal time pair and density correlations already give considerable insight into the effect of disorder on superconductivity. The long-range pairing order in the ground state is suppressed to zero for disorder $V\sim4t$, when $U=-4t$. Off half filling, the charge correlations are small and little affected by randomness, though disorder does cause an enhancement of the double occupancy rate. However, considerably more information can be obtained by looking also at various imaginary time-dependent quantities such as the current-current correlation function.

VI. CURRENT-CURRENT CORRELATION FUNCTION

As known for some time,[43] and also described recently in the context of quantum simulations,[44] various limits of the current–current correlation function give information about the charge and superfluid stiffness, and gauge invariance, and in principle can be used to distinguish insulators, metals, and superconductors. The current-current correlation function $\Lambda_{xx}(\mathbf{l},\tau)$ is defined by

$$\Lambda_{xx}(\mathbf{l},\tau)=\langle j_x(\mathbf{l},\tau)j_x(0,0)\rangle,$$
$$j_x(\mathbf{l}\tau)=e^{H\tau}\left[it\sum_{\sigma}\left(c^{\dagger}_{\mathbf{l}+\hat{x},\sigma}c_{\mathbf{l},\sigma}-c^{\dagger}_{\mathbf{l},\sigma}c_{\mathbf{l}+\hat{x},\sigma}\right)\right]e^{-H\tau}. \tag{11}$$

Upon Fourier transforming in space and imaginary time we get $\Lambda_{xx}(\mathbf{q},\omega_n)=\Sigma_{\mathbf{l}}\int_0^{\beta}d\tau e^{i\mathbf{q}\cdot\mathbf{l}}e^{-i\omega_n\tau}\Lambda_{xx}(\mathbf{l},\tau)$, where $\omega_n=2n\pi/\beta$.

A. Longitudinal response

The longitudinal part of Λ_{xx} defined in Eq. (11) must satisfy the *f*-sum rule,

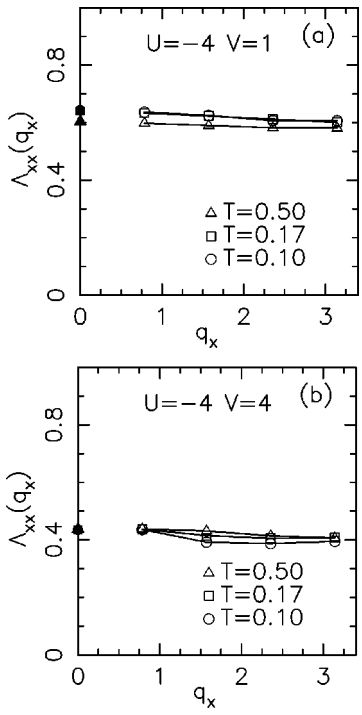

FIG. 6. The longitudinal current-current correlation function $\Lambda_{xx}(q_x)$ defined in Eq. (12) as a function of q_x at $T=0.5t$ (open triangles), $0.17t$ (open squares), and $0.1t$ (open circles). The corresponding filled points at $q_x=0$ are the magnitude of the kinetic energy K_x along x at those temperatures. In (a) $V=1t$ and in (b) $V=4t$. In all cases $\Lambda^{\mathrm{L}}=\Lambda_{xx}(q_x\rightarrow0)$ approaches K_x as required by gauge invariance.

$$\Lambda^{\mathrm{L}}\equiv\lim_{q_x\rightarrow0}\Lambda_{xx}(q_x,q_y=0,\omega_n=0),$$
$$\Lambda^{\mathrm{L}}=K_x, \tag{12}$$

as a consequence of gauge invariance.[43,44] Here $K_x=\langle t\Sigma_{\sigma}(c^{\dagger}_{\mathbf{l}+\hat{x},\sigma}c_{\mathbf{l},\sigma}+c^{\dagger}_{\mathbf{l},\sigma}c_{\mathbf{l}+\hat{x},\sigma})\rangle$ is the magnitude of the kinetic energy in the x direction.

Figure 6 shows $\Lambda_{xx}(q_x)$ as a function of q_x for different temperatures at weak disorder $V=1t$ [in (a)] and at strong disorder $V=4t$ [in (b)]. In both cases one finds that $\Lambda^{\mathrm{L}}\equiv\Lambda_{xx}(q_x\rightarrow0)=K_x$ at all T, verifying the gauge invariance condition and providing a nontrivial check of our numerics.

B. Transverse response: Superfluid stiffness

The transverse response is given by

$$\Lambda^{T}\equiv\lim_{q_y\rightarrow0}\Lambda_{xx}(q_x=0,q_y,\omega_n=0). \tag{13}$$

In a system with a broken gauge symmetry, the longitudinal and transverse responses are no longer equal and their difference is precisely the superfluid stiffness D_s or the related quantity, superfluid density ρ_s, given by

$$\rho_s=D_s/\pi=[\Lambda^{\mathrm{L}}-\Lambda^{\mathrm{T}}]=[K_x-\Lambda^{\mathrm{T}}]. \tag{14}$$

It can be seen from Eq. (14) that on a lattice the superfluid density at $T=0$ is indeed bounded above by the kinetic energy. In recent work[12] we have obtained an improved upper bound on D_s in a disordered system in terms of the local

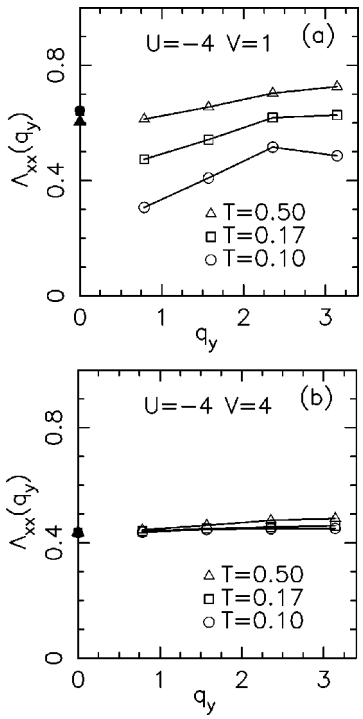

FIG. 7. The transverse current-current correlation function $\Lambda_{xx}(q_y)$ defined in Eq. (13) as a function of q_y at $T=0.5t$ (open triangles), $0.17t$ (open squares), and $0.1t$ (open circles). The corresponding filled points at $q_y=0$ are the magnitude of the kinetic energy along x at those temperatures. For weak disorder $V=1t$ as in (a), $\Lambda^T=\Lambda_{xx}(q_y\to 0)<K_x$ indicating the development of a finite superfluid stiffness D_s from Eq. (14) with decreasing T. For strong disorder $V=4t$ as in (b), $D_s=0$ at all T.

kinetic energy that highlights the dominance of the weak links in determining the superfluid stiffness.

In order to extract the superfluid stiffness D_s from Eq. (14) we must extrapolate $\Lambda_{xx}(q_y)$ to $q_y\to 0$. Using general symmetry arguments we have

$$j_\alpha(\mathbf{q})=\Lambda_{\alpha\beta}(\mathbf{q})A_\beta(\mathbf{q}),$$
$$\Lambda_{\alpha\beta}=\left(\delta_{\alpha\beta}-\frac{q_\alpha q_\beta}{q^2}\right)\Lambda^T(q^2)+\frac{q_\alpha q_\beta}{q^2}\Lambda^L(q^2), \tag{15}$$

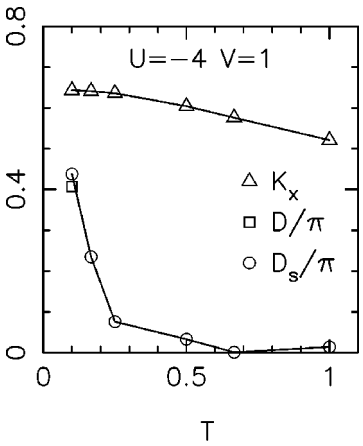

FIG. 8. The superfluid stiffness D_s and K_x as a function of T for $V=1.0$, $U=-4t$, and $\langle n\rangle=0.875$. Also shown is the charge stiffness D at the lowest $T=0.1$.

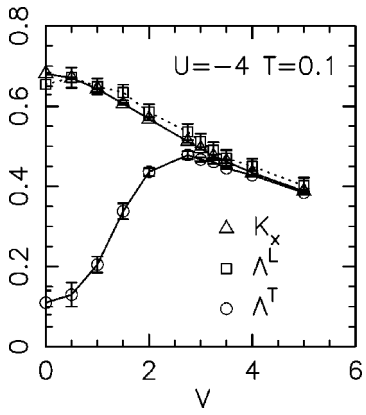

FIG. 9. The transverse current-current correlation function $\Lambda^T=\lim_{q_y\to 0}\Lambda_{xx}(q_y)$ as a function of disorder at $T=0.10$. Also shown is $K_x=\Lambda^L$, the longitudinal response function, as a function of disorder. The difference between Λ^L and Λ^T is the superfluid stiffness as seen from Eq. (14).

so that the linear term in the expansion of Λ^T and Λ^L is absent and the lowest-order term is quadratic in q_y. However, the momentum discretization on an 8×8 lattice is too coarse to see this quadratic behavior.

It is clear from Fig. 7 that the transverse correlations behave quite differently from the longitudinal correlations. For weak disorder, at high temperature, Λ^T approaches K_x, but as T is decreased, the two quantities no longer match, indicating that a nonzero superfluid density is developing as shown in Fig. 8. We see that D_s becomes significantly different from zero at temperatures $T<0.2t$. This is consistent with estimates[35] that put $T_c\approx 0.1t$ based on a finite-size scaling analysis of the pairing correlations, but seems to contradict recent suggestions that T_c is much lower, approximately $0.03t$. In Fig. 8 we also show the behavior of K_x that shows no special features as T is lowered. K_x declines from 0.68 at $V=0$ to $0.39t$ at $V=5t$, while D_s changes by almost two orders of magnitude. While a reduction in hopping is expected in the presence of disorder, the smooth behavior of the kinetic energy emphasizes that such a local quantity cannot serve as an order parameter for the localization transition. When disorder is strong, Λ^T remains pinned at K_x, for all T, suggesting that a superconducting phase is not present.

Thus from the raw data itself there is compelling evidence for a superconducting phase at low temperature and at low disorder that is qualitatively distinct from the nonsuperconducting phase at higher disorder.

Finally, we note that the mean-field gap is of the order of the hopping integral t for $U=-4t$, therefore quasiparticle excitations across the gap are suppressed by a factor $\sim\exp(-t/T)=\exp(-10)$ at a temperature $T=0.1t$. The finite temperature transition is thus dominated largely by thermal phase fluctuations.

C. Superconductor-insulator transition

In order to determine the location of the transition, we now present data at a set of disorder values that sweeps through the values $V=1-4$ that we argued in the preceding section brackets the transition. In Fig. 9 we show the extrapolated values of $\Lambda_{xx}(q_y)$ and K_x as a function of disor-

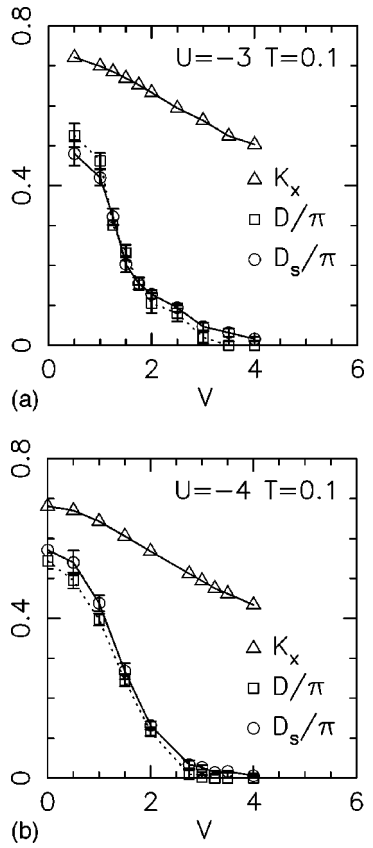

FIG. 10. The superfluid stiffness D_s and the charge stiffness D as a function of disorder strength V for $U=-3t$ and $U=-4t$. Note the rapid suppression with disorder and the transition from a superconductor to an insulator beyond a critical disorder.

der. It is evident that the transition is driven by the variation of Λ^T. In Fig. 10 we show D_s as a function of disorder strength at fixed temperature $T=0.1t$, for $U=-3t$ and $U=-4t$. The decrease in D_s with increasing disorder is consistent with the decline in the order parameter shown in Fig. 5.

The superfluid stiffness $D_s \sim \delta^{\zeta}$, where $\delta=|V-V_c|/|V_c|$ is the distance from critical disorder. The exponent ζ is expected to be larger than unity since $\zeta=z\nu$ and in two dimensions it has been argued that $\nu \geqslant 2/d=1$ and $z=2$. A value of $\zeta>1$ implies that the finite-size rounding will shift the critical point on the infinite lattice to *higher* values compared to the point where D_s becomes small on finite lattices. So we expect that the critical point for the SIT may lie around $V_c \approx 3-4t$ for $U=-4t$.

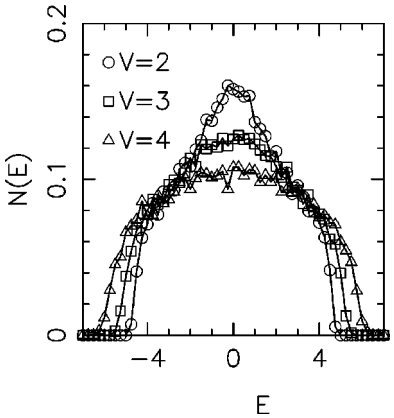

FIG. 11. The density of states $N(E)$ as a function of energy E for noninteracting fermions ($U=0$) on an 8×8 lattice at density $\langle n\rangle=0.875$ for disorder strengths around $V=2t$, $3t<V_c$, and $V=4t>V_c$, where V_c is the critical disorder of the interacting problem with $U=-4t$.

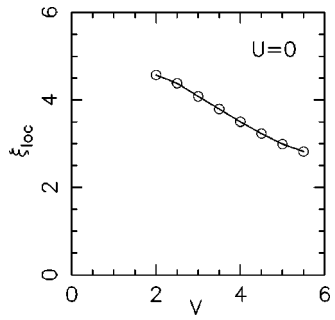

FIG. 12. The approximate localization length of the eigenstate at the Fermi surface inferred from the participation ratio by as a function of disorder strength V. We see that the single-particle eigenstates do not show any sharp behavior around the critical disorder $V_c \sim 3.25$ found for the SIT in our QMC simulations of the interacting problem.

It is reasonable to ask to what extent the sharp drop in the pair correlations and the transition to insulating behavior in the resistivity might reflect changes in the noninteracting eigenstates of the Hamiltonian. Is the fact that the pairing correlations are robust at $V=0$ but zero at $V=5t$ a consequence of some changes in the extent of the single-particle wave functions due to disorder?

In Fig. 11 we show the density of states $N(E)$ for $U=0$ and different amounts of randomness bracketing V_c. We see that disorder broadens $N(E)$, as expected, but the behavior of this quantity through V_c is smooth.

We show in Fig. 12 the localization length or the ''size'' of the eigenstate at the Fermi surface, defined by $\xi_{loc}=\sqrt{\mathcal{P}R(E_F)}$ as a function of disorder strength. ξ_{loc} shows a smooth decrease as a function of V, without any sharp feature at V_c. We conclude that the SIT is not occurring as a consequence of a $U=0$ Anderson transition on the finite lattice, even though the wave functions are localized on the scale of the linear lattice size L. Instead, the transition is a genuinely nontrivial many-body effect.

D. Coherence length

In principle, we can extract the superconducting coherence length ξ for the many-body problem from the dependence of $\Lambda^T(q_y)=a+bq_y^2$ for small q_y. From Eq. (14) we see that

$$\frac{D_s(q_y)}{\pi}=\frac{D_s}{\pi}[1-q_y^2\xi^2], \tag{16}$$

where $\xi^2=b/(D_s/\pi)$. As a function of disorder ξ is found to decrease slightly for low disorder and is expected to diverge as the critical disorder is approached. However, it is difficult to deduce such a divergence from the data since both b and D_s are becoming small near the transition. Further work on

this problem is required, since it would be useful to obtain the coherence length to track the quantum phase transition.

VII. CHARGE STIFFNESS

A superconductor is characterized by the Meissner effect, measured by the superfluid stiffness, as well as by an infinite conductivity. A signature of the latter is a delta function in the optical conductivity

$$\mathrm{Re}\,\sigma(\omega)=D\,\delta(\omega)+\mathrm{Re}\,\sigma_{reg}(\omega) \tag{17}$$

with weight $D=\pi[K_x-\lim_{\omega\to 0}\ \mathrm{Re}\ \Lambda_{xx}(\mathbf{q}=0;\omega+i0^+)]$, known as the charge stiffness. The regular part of the conductivity is given by (suppressing the $\mathbf{q}=0$ and omitting the xx subscripts)

$$\mathrm{Re}\,\sigma_{\mathrm{reg}}(\omega)=\frac{\mathrm{Im}\,\Lambda(\omega)}{\omega}, \tag{18}$$

where $\Lambda(\omega+i0^+)=\mathrm{Re}\,\Lambda(\omega)+i\,\mathrm{Im}\,\Lambda(\omega)$.

In order to obtain the dc limit we proceed as follows. We start with the sum rule

$$\int_0^\infty d\omega\,\mathrm{Re}\,\sigma(\omega)=\frac{\pi}{2}K_x \tag{19}$$

and combine with Eq. (17) to get

$$\int_0^\infty d\omega\mathrm{Re}\,\sigma_{reg}(\omega)=\frac{\pi}{2}K_x-\frac{D}{2}. \tag{20}$$

Next, using the spectral representation for $\Lambda(z)$,

$$\Lambda(z)=\int_{-\infty}^{\infty}\frac{d\omega}{\pi}\frac{\mathrm{Im}\,\Lambda\ (\omega)}{\omega-z}, \tag{21}$$

and substituting $z=i\omega_n$ we get

$$\Lambda(\omega_n)=\frac{2}{\pi}\int_0^\infty d\omega\,\frac{\omega\,\mathrm{Im}\,\Lambda\ (\omega)}{\omega^2+\omega_n^2}. \tag{22}$$

Using Eq. (18),

$$\Lambda(\omega_n)=\frac{2}{\pi}\int_0^\infty d\omega\mathrm{Re}\,\sigma_{\mathrm{reg}}(\omega)\\ -\frac{2}{\pi}\omega_n^2\int_0^\infty d\omega\frac{\mathrm{Re}\,\sigma_{\mathrm{reg}}(\omega)}{\omega^2+\omega_n^2}. \tag{23}$$

Substituting for the first term from Eq. (20) and defining the Matsubara correlation function

$$D(\omega_n)=\pi[K_x-\Lambda(\omega_n)], \tag{24}$$

whence

$$D(\omega_n)=D+2\omega_n^2\int_0^\infty d\omega\,\frac{\sigma_{\mathrm{reg}}(\omega)}{[\omega^2+\omega_n^2]}. \tag{25}$$

The behavior of $\Lambda(\omega_n)$ as a function of n is shown in Fig. 13 for low disorder $V=1t$ in (a) and for high disorder $V=4t$ in (b). The behavior of $\Lambda(\omega_n)$ is qualitatively similar to Fig. 7. That is, at strong disorder $\Lambda(\omega_n\to 0)\approx K_x$ at all temperatures and according to Eq. (24) this implies the charge stiffness $D\approx 0$, as is the superfluid stiffness D_s. At weak disorder and at low T on the other hand, $\Lambda(\omega_n\to 0)<K_x$, implying that D is nonzero. In Fig. 14 we show $D(\omega_n)$ as a function of n that is found to increase monotonically with n

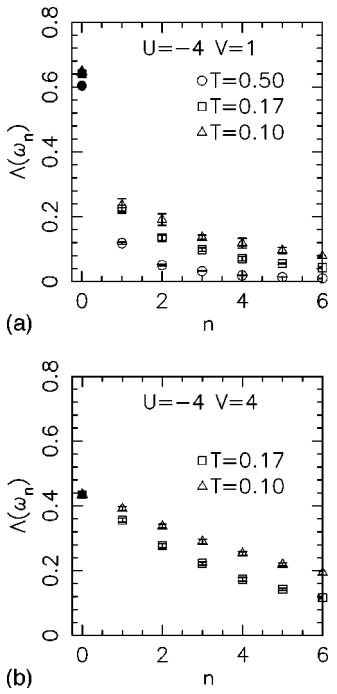

FIG. 13. The behavior of $\Lambda(\omega_n)$ as a function of n at temperatures $T=$ 0.17 and 0.10. The corresponding filled points at $n=0$ are the values of K_x at those temperatures. For weak disorder $V=t$ $\lim_{\omega_n\to 0}\Lambda(\omega_n)<K_x$ indicating a finite charge stiffness D whereas at strong disorder $V=4t$, $\lim_{\omega_n\to 0}\Lambda(\omega_n)\approx K_x$, implying that $D=0$.

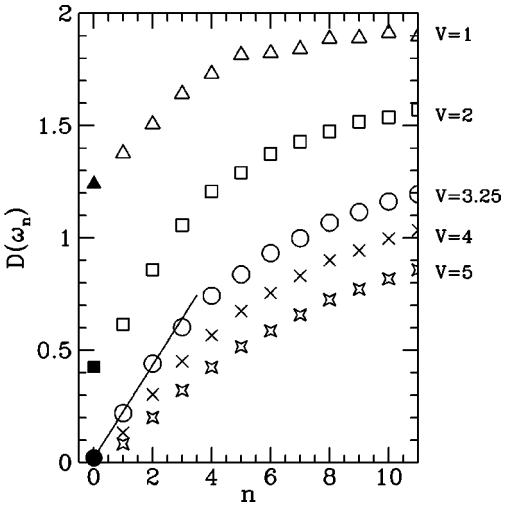

FIG. 14. The behavior of $D(\omega_n)$ defined in Eq. (24) as a function of n for $T=0.1$, $U=-4t$, and $\langle n\rangle=0.875$ for disorder strengths $V=1,2,3.25,4,5t$. The corresponding filled points at $\omega_n=0$ are the extrapolated values of the charge stiffness D at those V. The critical disorder $V_c=3.25$ is identified by the vanishing of $D(\omega_n)$. The straight line is a linear fit to the low ω_n data whose slope is proportional to the critical conductivity at the transition from Eq. (29).

from $D(\omega_n \to 0) = D$ to $D(\omega_n \to \infty) = \pi(-K_x)$ (not shown in the figure) but verified in the data.

The behavior of D as a function of disorder extracted from Eq. (25) is shown in Fig. 10. We see that D and D_s are within 10–20 % of each other for all the parameters shown. Thus there is remarkable consistency between the superfluid stiffness D_s and the strength D of the delta function in the optical conductivity, obtained from two very different correlation functions.

Do these techniques give sensible results in the noninteracting, clean limit? For $U=V=0$ we find the charge stiffness $D/\pi = 0.79 = \langle -K_x \rangle$ whereas the superfluid stiffness $D_s/\pi = 0.0243$ for filling $\langle n \rangle = 0.86$ and $T = 0.1t$ on an 8×8 system. Thus our numerics are correctly telling us that free fermions are metallic with a nonzero D, but a very small D_s, which will go to zero as the system size increases.

While the approximate equality of D and D_s in Fig. 10 for a superconductor is a good check on the calculation, it emphasizes that the charge stiffness D at $T=0$ cannot be used to characterize the nonsuperconducting state for $V \geqslant V_c$ since neither dirty metals nor insulators have a δ function in $\sigma(\omega)$ at $\omega = 0$. Hence we turn to the conductivity.

VIII. CONDUCTIVITY

The dc conductivity $\sigma_{dc} = \lim_{\omega \to 0} \mathrm{Re}\, \sigma_{reg}(\omega)$ defined in Eq. (18) is of considerable theoretical and experimental interest as it distinguishes the two nonsuperconducting phases—metal (above T_c) vs insulator. The fluctuation-dissipation theorem relates $\mathrm{Im}\Lambda(\omega)$ that is required for the calculation of σ_{dc} to $\Lambda(\tau)$ that is obtained from QMC data by

$$\Lambda(\tau) = \int_{-\infty}^{+\infty} \frac{d\omega}{\pi} \frac{\exp(-\omega\tau)}{[1-\exp(-\beta\omega)]} \mathrm{Im}\,\Lambda(\omega), \qquad (26)$$

valid for $0 \leqslant \tau \leqslant \beta$. However, the evaluation of $\mathrm{Im}\,\Lambda(\omega)$ requires an analytic continuation of noisy imaginary time data, which is difficult. We derive below an approximate expression for σ_{dc},[22] analogous to that introduced previously for the susceptibility,[24] by noting that if one sets $\tau = \beta/2$, the kernel in Eq. (26) cuts off contributions from high frequencies, and the important range of ω is restricted to increasingly small values as β becomes large. Therefore, at low enough temperatures one might replace

$\mathrm{Im}\,\Lambda(\omega) \simeq \omega\sigma_{\mathrm{dc}}$ over the entire range of integration, which leads to the result

$$\sigma_{\mathrm{dc}} = \frac{\beta^2 \Lambda(\tau = \beta/2)}{\pi}. \qquad (27)$$

Note that Eq. (27) is only valid in the normal state ($T_c \approx 0.1t$) where $\mathrm{Im}\,\Lambda(\omega) \sim \omega\sigma_{\mathrm{dc}}$ at low frequencies. We will present a number of self-consistent checks of Eq. (27) in the metallic state above T_c of the superconductor and the localized phase. We defer a discussion of the extraction of the conductivity at the SIT to the next section.

If Fig. 15 we show the behavior of the resistivity $\rho = 1/\sigma_{\mathrm{dc}}$ obtained from Eq. (27) as a function of temperature. The resistivity shows a behavior qualitatively similar to that seen in experiment: when the control parameter, in this case disorder, is weak, the behavior is metallic and ρ decreases as

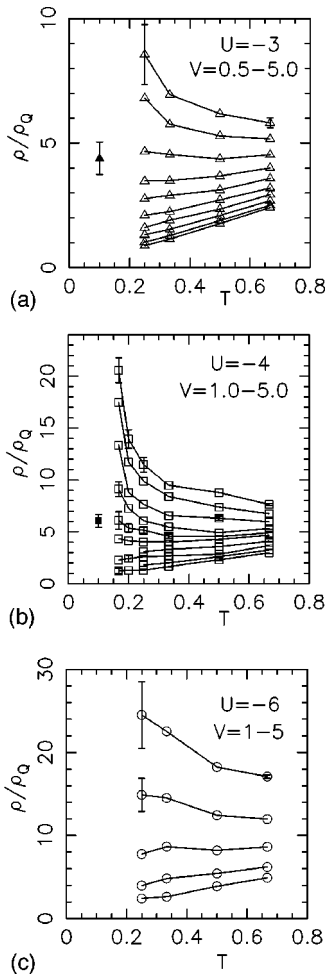

FIG. 15. The behavior of the resistivity ρ obtained from Eq. (27) as a function of T for various disorder strengths. These figures correspond to $U = -3, -4, -6$, respectively.

T decreases. On the other hand, for strong disorder, the behavior is insulating and ρ increases as T decreases. Our plots are qualitatively similar to those observed experimentally, though the experimental range of resistivities is much greater.

As is often done experimentally, data for $\rho(T)$ at different V can be replotted to show $\rho(V)$ for different temperatures. For $V < V_c$ the resistivity decreases as T is lowered, while for $V > V_c$ the resistivity increases as T is lowered. This leads to a characteristic crossing pattern in $\rho(V)$ that allows for an estimation of the critical amount of disorder V_c as well as the critical resistance $\rho(V_c)$ at the transition. Note that the crossing pattern does not follow from any deep scaling principle. Instead, it is merely a consequence of the monotonicity of the plots of $\rho(T)$ for a given V, which, to within error bars, either steadily increase or decrease as T is changed.

From Fig. 10 and Fig. 16 we see clear evidence for a SIT at a critical disorder $V_c(U)$ whose dependence on the strength of the attraction is shown in Fig. 17.

It has recently been emphasized by Sachdev[45] that using Eq. (27) to extract the resistivity is not applicable near a quantum phase transition as there is *no scale in the problem.* Note that it was assumed in the derivation of Eq. (27) that below some scale that was independent of T, it was possible to assume that $\mathrm{Im}\,\Lambda(\omega) \sim \omega\sigma_{\mathrm{dc}}$. This assumption breaks

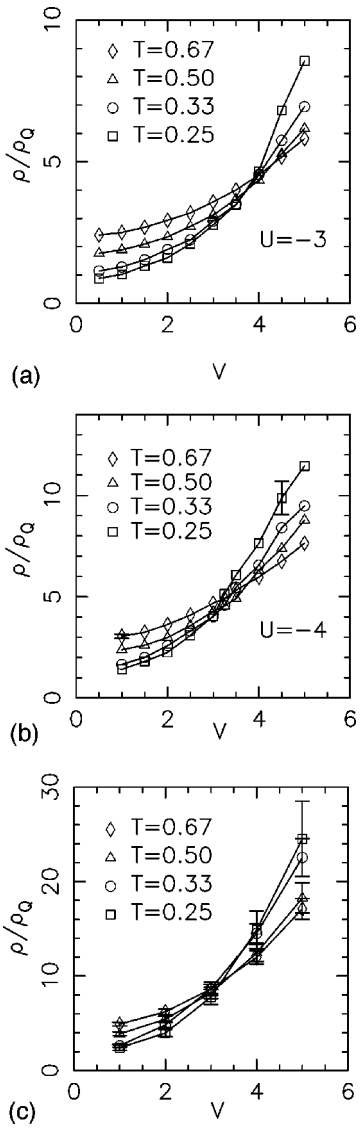

FIG. 16. The behavior of the resistivity ρ obtained from Eq. (27) as a function of V for various temperatures. These figures correspond to $U=-3,-4,-6$, respectively.

down near a quantum critical point since by definition all scales become soft. Away from the transition, Eq. (27) gives a good description of $\rho_{dc}(T)$; however, close to the transition, it cannot be used to extract the critical conductivity. The agreement of the transition point obtained by the conductivity crossing plots and the measurements of the superfluid and charge stiffness suggest that Eq. (27) has a useful range of validity.

We discuss another potential method to extract the conductivity at the critical point. As seen in Fig. 14 at a critical disorder D vanishes. At this disorder assume that $\mathrm{Re}\,\sigma(\omega) \rightarrow \sigma_0 = \text{const}$, for frequencies $\omega < \omega_c$, a cutoff value.

Then from Eq. (25)

$$D(\omega_n) = 2\omega_n^2 \int_0^\infty d\omega \frac{\sigma_{\mathrm{reg}}(\omega)}{\omega^2+\omega_n^2}$$

$$= 2\sigma_0 |\omega_n| \tan^{-1}\left(\frac{\omega_c}{\omega_n}\right) + 2\omega_n^2 \int_{\omega_c}^\infty d\omega \frac{\mathrm{Re}\,\sigma(\omega)}{\omega^2+\omega_n^2}, \tag{28}$$

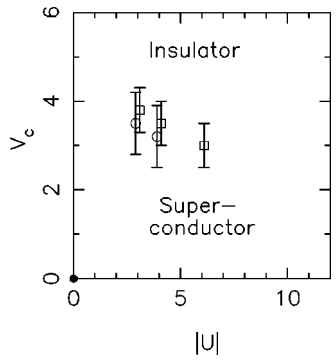

FIG. 17. The locus of critical disorder $V_c(U)$ for intermediate couplings in the disorder-V–attraction-$|U|$ plane. The V_c values are obtained by two independent methods, the vanishing of superfluid density D_s (open circles), and the crossing of the resistivity ρ (open squares). The filled circle at $U=V=0$ emphasizes that all noninteracting states are localized for any nonzero disorder V in two dimensions.

which in the limit of small Matsubara frequencies is given by

$$D(\omega_n) = \pi\sigma_0|\omega_n| + \mathcal{O}(\omega_n)^2. \tag{29}$$

The conductivity at the critical point obtained from Eq. (29) and from the crossing of the resistivity curves described above are in agreement to about 10%.

Near a quantum critical point, we expect

$$\sigma_{reg}(\omega, T, V=V_c) = \sigma_Q \sigma(\omega/T). \tag{30}$$

From Eq. (25), this implies that

$$\frac{D(\omega_n)}{T} = \frac{D(T)}{T} + 8\pi^2 n^2 \sigma_Q \int_{x_c}^\infty dx \frac{f(x)}{x^2+4\pi^2 n^2}$$

$$\equiv G(T) + F(n), \tag{31}$$

where $x=\omega/T$. Thus $D(\omega_n)/T$ is a sum of two terms; the first one $G(T)=D(T)/T$ is only a function of T and the second term $F(n)$ is only a function of n, with $F(n\rightarrow 0)=0$. We set $V=V_c\sim 3.25t$ and by extrapolating the behavior of $D(\omega_n)/T$ to $n\rightarrow 0$ obtain $G(T)$. In Fig. 18, we show the behavior of $F(n)$ vs $n=\omega_n/2\pi T$ at the critical point for various temperatures. The data are not found to scale, unlike our expectations at a critical point. Instead if we plot $D(\omega_n)$ vs ω_n we see a remarkable scaling behavior of the data for

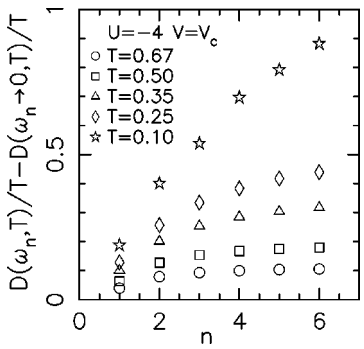

FIG. 18. The behavior of $F(n)=D(\omega_n,T)/T-D(\omega_n\rightarrow 0,T)/T$ as a function of $n=\omega_n/(2\pi T)$ defined in Eq. (31) at the critical disorder $V_c\sim 3.25t$ and various T.

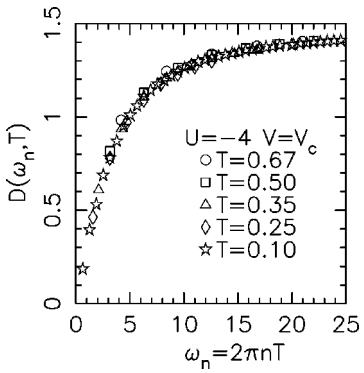

FIG. 19. The behavior of $D(\omega_n, T)$ as a function of ω_n at the critical disorder $V_c \sim 3.25t$ and various T.

various temperatures as seen in Fig. 19. It is not really clear as to why the data when plotted as in Fig. 18 do not scale.

It has been claimed in Ref. 46 that since in QMC the lowest frequency that can be accessed is $\omega_1 = 2\pi T > T$, it is not possible to extract the dc resistivity using Eq. (29) in the low-frequency limit. While this objection appears very sound, it is nevertheless the case that the conductivity inferred from Eq. (29), including its values in the vicinity of the critical point, is consistent with many other, completely rigorously founded, aspects of our simulation. By this we mean that the location of the transition inferred from the analysis of the data using Eq. (29) is in remarkable agreement with the location obtained from the superfluid stiffness D_s, and the charge stiffness D. Furthermore, the value of the conductivity at the transition is consistent with the value obtained from Eq. (27). At present we do not understand fully why the method appears to be so consistent with our other data despite the objections raised in Ref. 46.

IX. CONCLUSIONS

We have studied the effect of disorder on an *s*-wave superconductor of fixed coupling strength (modeled as an attractive Hubbard model away from half filling). We have found that with increasing disorder, the superfluid stiffness (obtained from the transverse current-current correlation function) and the charge stiffness (obtained from the τ-dependent current-current correlation function), vanish at a critical disorder, signaling a transition to a localized phase. The importance of our work lies in the fact that the SIT that has been observed experimentally, has eluded all mean-field treatments of the problem. Ours is the first theoretical study of a fermionic model to obtain a *transition* between the superconductor and localized phases upon increasing the disorder strength.

X. OUTSTANDING QUESTIONS

Having established the existence of the SIT the outstanding questions now relate to obtaining a quantitative characterization of the transition. For this it is necessary to perform finite-size scaling in both the spatial ($L \to \infty$) and the temporal ($T \to 0$) dimensions to obtain the location of the critical disorder from the vanishing of the superfluid stiffness D_s as well as the vanishing of the charge stiffness D. From the scaling of the data it is then possible to extract the dynamical exponent z and the correlation length exponent ν. Such an analysis will tell us whether the fermion SIT is in the same universality class as the bosonic superfluid-insulator transition or not. While there have been several studies of the superfluid-insulator transition[47,48] in the boson Hubbard model[49,50,18] and its variants,[17] we believe that the situation with regard to the value of the exponents is still unclear.[51] This is largely because of the complications of finite-size scaling analysis inherent in a quantum phase transition that necessarily involves two variables (system size $L \to \infty$ and temperature $T \to 0$).

Once the location and exponents characterizing the transition are determined, the key question is the value of the resistivity at the transition and the possibility of its universality. There is some experimental evidence that despite the wide range of materials and control parameters, the value of the resistance right at the transition R^* is always quite close to the ''universal'' value[2,3,5,4] $R_Q = h/4e^2$. While there is still some debate concerning whether this number is truly the same for all systems, it is certainly clear that the variation in R^* is much less than the variations in the location of the transition in other control parameters such as the temperature, magnetic field strength, or film thickness. Recent experiments of Yazdani and Kapitulnik[6] have interpreted the variation in R^* that exists in terms of separate bosonic and fermionic contributions to the resistivity. Thus, calculations with models that include electronic degrees of freedom like the attractive Hubbard Hamiltonian are needed to supplement work on bosonic theories. To address this set of issues concerning R^*, we require an exact method to calculate the resistivity at the transition, as would be provided by maximum entropy techniques. We are currently working on this problem.

ACKNOWLEDGMENTS

We would like to thank M. Randeria and S. Sachdev for many useful discussions. We also thank K. Runge for providing useful scripts for doing the disorder averaging. The numerical calculations were performed at the NCSA. This work was supported by the NSF under Grant No. DMR95-28535 (R.T.S.).

[1] See review article by A. F. Hebard, in *Strongly Correlated Electronic Systems*, edited by K. S. Bedell, Z. Wang, D. E. Meltzer, A. V. Balatsky, and E. Abrahams (Addison-Wesley, Reading, MA, 1994).

[2] D. B. Haviland, Y. Liu, and A. M. Goldman, Phys. Rev. Lett. **62**, 2180 (1989).

[3] R. C. Dynes, J. P. Garno, G. B. Hertel, and T. P. Orlando, Phys. Rev. Lett. **53**, 2437 (1984); A. E. White, R. C. Dynes, and J. P. Garno, Phys. Rev. B **33**, 3549 (1986).

[4] J. M. Valles, R. C. Dynes, and J. P. Garno, Phys. Rev. Lett. **69**, 3567 (1992).

[5] A. F. Hebard and M. A. Paalanen, Phys. Rev. Lett. **65**, 927 (1990); M. A. Paalanen, A. F. Hebard, and R. R. Ruel, *ibid.* **69**, 1604 (1992).

[6] A. Yazdani and A. Kapitulnik, Phys. Rev. Lett. **74**, 3037 (1995); J. M. Graybeal and M. R. Beasley, Phys. Rev. B **29**, 4167 (1984).
[7] A. G. Sun, L. M. Paulius, D. A. Gajewski, M. B. Maple, and R. C. Dynes, Phys. Rev. B **50**, 3266 (1994).
[8] G. T. Seidler, T. F. Rosenbaum, and B. W. Veal, Phys. Rev. B **45**, 10 162 (1992).
[9] L. J. Geerligs, M. Peters, L. E. M. de Groot, A. Verbruggen, and J. E. Mooij, Phys. Rev. Lett. **63**, 326 (1989); J. E. Mooij, B. J. van Wees, L. J. Geerligs, M. Peters, R. Fazio, and G. Schön, *ibid.* **65**, 645 (1990).
[10] P. W. Anderson, J. Phys. Chem. Solids **11**, 26 (1959).
[11] M. Ma and P. A. Lee, Phys. Rev. B **32**, 5658 (1985).
[12] A. Paramekanti, N. Trivedi, and M. Randeria, Phys. Rev. B **57**, 11 639 (1998).
[13] M. P. A. Fisher, G. Grinstein, and S. M. Girvin, Phys. Rev. Lett. **64**, 587 (1990).
[14] A. M. Finkelstein, Physica B **197**, 636 (1994).
[15] D. Belitz and T. Kirkpatrick, Rev. Mod. Phys. **66**, 261 (1994).
[16] M. Cha, M. P. A. Fisher, S. M. Girvin, M. Wallin, and A. P. Young, Phys. Rev. B **44**, 6883 (1991).
[17] E. S. Sorensen, M. Wallin, S. M. Girvin, and A. P. Young, Phys. Rev. Lett. **69**, 828 (1992).
[18] K. J. Runge, Phys. Rev. B **45**, 13 136 (1992).
[19] G. G. Batrouni, B. Larson, R. T. Scalettar, J. Tobochnik, and J. Wang, Phys. Rev. B **48**, 9628 (1993).
[20] A. Ghosal, M. Randeria, and N. Trivedi, Phys. Rev. Lett. **81**, 3940 (1998).
[21] C. Huscroft and R. T. Scalettar, Phys. Rev. Lett. **81**, 2775 (1998).
[22] N. Trivedi, R. T. Scalettar, and M. Randeria, Phys. Rev. B **54**, 3756 (1996).
[23] C. Huscroft and R. T. Scalettar, Phys. Rev. B **55**, 1185 (1997).
[24] M. Randeria, N. Trivedi, A. Moreo, and R. T. Scalettar, Phys. Rev. Lett. **69**, 2001 (1992).
[25] N. Trivedi and M. Randeria, Phys. Rev. Lett. **75**, 312 (1995).
[26] N. Trivedi and M. Randeria, J. Supercond. **9**, 13 (1996).
[27] M. Randeria and J. C. Campuzano, in *Models and Phenomenology for Conventional and High Temperature Superconductors*, Proceedings of the International School of Physics ''Enrico Fermi,'' Course CXXXVI, edited by G. Iadonisi, J. R. Schrieffer, and M. L. Chiofalo (North-Holland, Amsterdam, 1998).
[28] M. Randeria and N. Trivedi, J. Phys. Chem. Solids (to be published).
[29] M. Randeria, in *Bose Einstein Condensation*, edited by A. Giffin *et al.* (Cambridge University Press, Cambridge, 1994).
[30] N. Trivedi, R. T. Scalettar, and M. Randeria, Indian J. Pure Appl. Phys. **34**, 734 (1996).
[31] R. T. Scalettar. P. J. Denteneer, C. Huscroft, A. McMahan, R. Pollock, M. Randeria, N. Trivedi, and G. T. Zimanyi, Mater. Res. Bull. (to be published).
[32] R. T. Scalettar, E. Y. Loh, Jr., J. E. Gubernatis, A. Moreo, S. R. White, D. J. Scalapino, R. L. Sugar, and E. Dagotto, Phys. Rev. Lett. **62**, 1407 (1989); A. Moreo, D. J. Scalapino, R. L. Sugar, S. R. White, and N. E. Bickers, Phys. Rev. B **41**, 2313 (1990).
[33] R. Micnas, J. Ranninger, and S. Robaszkiewicz, Rev. Mod. Phys. **62**, 113 (1990).
[34] This is seen by performing a phased particle-hole transformation on the down-spin electrons that results in a mapping onto the repulsive model.
[35] A. Moreo and D. J. Scalapino, Phys. Rev. Lett. **66**, 946 (1991).
[36] P. J. H. Denteneer, Phys. Rev. B **49**, 6364 (1994); **53**, 9764 (1996).
[37] R. Blankenbecler, R. L. Sugar, and D. J. Scalapino, Phys. Rev. D **24**, 2278 (1981).
[38] D. J. Scalapino, in *High Temperature Superconductivity, Proceedings of the Los Alamos Symposium*, edited by K. S. Bedell (Addison-Wesley, Reading, MA, 1989).
[39] G. Sugiyama and S. E. Koonin, Ann. Phys. (N.Y.) **168**, 1 (1986); S. Sorella, S. Baroni, R. Car, and M. Parrinello, Europhys. Lett. **8**, 663 (1989); S. Sorella, E. Tosatti, S. Baroni, R. Car, and M. Parrinello, Int. J. Mod. Phys. B **1**, 993 (1989).
[40] S. R. White, D. J. Scalapino, R. L. Sugar, E. Y. Loh, Jr., J. E. Gubernatis, and R. T. Scalettar, Phys. Rev. B **40**, 506 (1989).
[41] J. Hirsch, Phys. Rev. B **28**, 4059 (1983).
[42] F. Pázmándi, R. T. Scalettar, and G. T. Zimányi, Phys. Rev. Lett. **79**, 5130 (1997).
[43] G. Baym, in *Mathematical Methods in Solid State and Superfluid Theory, Scottish Universities Summer School, 1967*, edited by R. C. Clark and G. H. Derrick (Plenum, New York, 1969).
[44] D. J. Scalapino, S. R. White, and S. C. Zhang, Phys. Rev. B **47**, 7995 (1993).
[45] S. Sachdev (private communication); For a general review, see S. Sachdev, in *Statistical Physics 19*, edited by Hao Bailin (World Scientific, Singapore, 1996).
[46] K. Damle and S. Sachdev, Phys. Rev. B **57**, 8307 (1998); cond-mat/9705206 (unpublished).
[47] M. P. A. Fisher, P. B. Weichman, G. Grinstein, and D. S. Fisher, Phys. Rev. B **40**, 546 (1989).
[48] For a review of bosons, see the article by G. T. Zimanyi, in *Strongly Correlated Electronic Materials*, edited by K. Bedell *et al.* (Addison-Wesley, Reading, MA, 1994), p. 285, and references cited therein.
[49] G. G. Batrouni, R. T. Scalettar, and G. T. Zimanyi, Phys. Rev. Lett. **65**, 1765 (1990); R. T. Scalettar, G. G. Batrouni, and G. T. Zimanyi, *ibid.* **66**, 3144 (1991).
[50] W. Krauth, N. Trivedi, and D. M. Ceperley, Phys. Rev. Lett. **67**, 2307 (1991); M. Makivic, N. Trivedi, and S. Ullah, *ibid.* **71**, 2307 (1993).
[51] N. Trivedi, Condens. Matter Theor. **12**, 141 (1997).